Neuron, Vol. 21, 123–136, July, 1998, Copyright ©1998 by Cell Press

Munc13-1 Is a Presynaptic Phorbol Ester Receptor that Enhances Neurotransmitter Release

Andrea Betz,*# Uri Ashery,†# Michael Rickmann,‡# Iris Augustin,* Erwin Neher,† Thomas C. Südhof,§ Jens Rettig,† and Nils Brose*‖
*Max-Planck-Institut für Experimentelle Medizin
Abt. Molekulare Neurobiologie
Hermann-Rein-Str. 3
D-37075 Göttingen
Bundesrepublik Deutschland
†Max-Planck-Institut für Biophysikalische Chemie
Abt. Membranbiophysik
Am Faßberg 11
D-37077 Göttingen
Bundesrepublik Deutschland
‡Universität Göttingen
Zentrum Anatomie
Abt. Neuroanatomie
Kreuzbergring 36
D-37075 Göttingen
Bundesrepublik Deutschland
§University of Texas Southwestern Medical Center
Howard Hughes Medical Institute
and Department of Molecular Genetics
Dallas, Texas 75235

Summary

Munc13-1, a mammalian homolog of *C. elegans* unc-13p, is thought to be involved in the regulation of synaptic transmission. We now demonstrate that Munc13-1 is a presynaptic high-affinity phorbol ester and diacylglycerol receptor with ligand affinities similar to those of protein kinase C. Munc13-1 associates with the plasma membrane in response to phorbol ester binding and acts as a phorbol ester–dependent enhancer of transmitter release when overexpressed presynaptically in the *Xenopus* neuromuscular junction. These observations establish Munc13-1 as a novel presynaptic target of the diacylglycerol second messenger pathway that acts in parallel with protein kinase C to regulate neurotransmitter secretion.

Introduction

Transmitter release from nerve cells is mediated by exocytosis. Synaptic vesicles, the key organelles in this process, undergo a complex cycle of fusion and fission events that regulate the release process in the synapse. Vesicles are generated by budding from early endosomes and are loaded with neurotransmitter. After a translocation process, they dock at the active zone and mature to a fusion competent state. In response to a rise in the intracellular calcium concentration, fusion competent vesicles release their content through exocytosis. Vesicular protein and membrane components are then retrieved by clathrin-mediated endocytosis and recycled via early endosomes (Südhof, 1995; Söllner and Rothman, 1996; Cremona and De Camilli, 1997; Hanson et al., 1997a; Hay and Scheller, 1997).

Membrane fusion and fission are the central reactions of the synaptic vesicle cycle and are likely to be mediated by a small set of essential proteins (Hanson et al., 1997b). Many more presynaptic proteins have regulatory functions, by conferring directionality and target specificity of the transport processes or by modulating essential steps of the synaptic vesicle cycle through protein–protein interactions (Südhof, 1995; Söllner and Rothman, 1996; Cremona and De Camilli, 1997; Hanson et al., 1997a; Hay and Scheller, 1997). Additional levels of modulation are provided by second messengers. These either act directly on protein components of the release machinery, like Ca^{2+} on the exocytotic calcium sensor synaptotagmin (Südhof and Rizo, 1996), or they activate regulatory enzymes such as protein kinases, which in turn modulate the function of presynaptic proteins via phosphorylation (Byrne and Kandel, 1996).

In particular, members of the protein kinase C (PKC) family of serine/threonine kinases have a prominent influence on neurotransmitter release by modifying ion channels and changing the ionic conductance of nerve cell membranes and/or by acting directly on the transmitter release apparatus (Dekker et al., 1991; Byrne and Kandel, 1996; Gillis et al., 1996). Apart from Ca^{2+}, which stimulates a subset of PKC isoforms, most PKCs are activated by diacylglycerol and, more potently, by the tumor-promoting phorbol esters (Newton, 1995, 1997). Both types of ligands bind to the regulatory C_1-domain of PKCs and serve as hydrophobic anchors that recruit the enzyme to the plasma membrane, stabilize its active conformation, and increase its susceptibility to other second messengers (Newton, 1995, 1997). As a consequence, phorbol esters were used as key reagents in a large number of studies examining the role of PKC in transmitter release and many other physiological processes. Almost invariably, their effects were attributed to PKC activation. However, phorbol esters also mediate PKC-independent effects on membrane traffic (Fabbri et al., 1994) and synaptic transmission (Scholfield and Smith, 1989; Redman et al., 1997), indicating the presence of additional diacylglycerol and phorbol ester targets involved in neuronal membrane traffic.

The family of unc-13p-like proteins constitutes a group of novel potential phorbol ester and diacylglycerol receptors that may be involved in synaptic signaling (Maruyama and Brenner, 1991; Brose et al., 1995; Betz et al., 1997). *Caenorhabditis elegans* unc-13p has an essential function in synaptic transmission: mutations in the *unc-13* locus lead to a severely paralyzed phenotype that was interpreted to reflect a perturbation of presynaptic processes (Hosono et al., 1987; Hosono and Kamiya, 1991). The primary structure of unc-13p is characterized by two C_2-domains homologous to the Ca^{2+}-binding regulatory region of PKCs and a zinc finger–like C_1-domain that binds phorbol esters with high affinity (Kazanietz et al., 1995). Munc13-1 and two closely related

‖To whom correspondence should be addressed (e-mail: brose@mail.mpiem.gwdg.de).
#These authors contributed equally to this work.

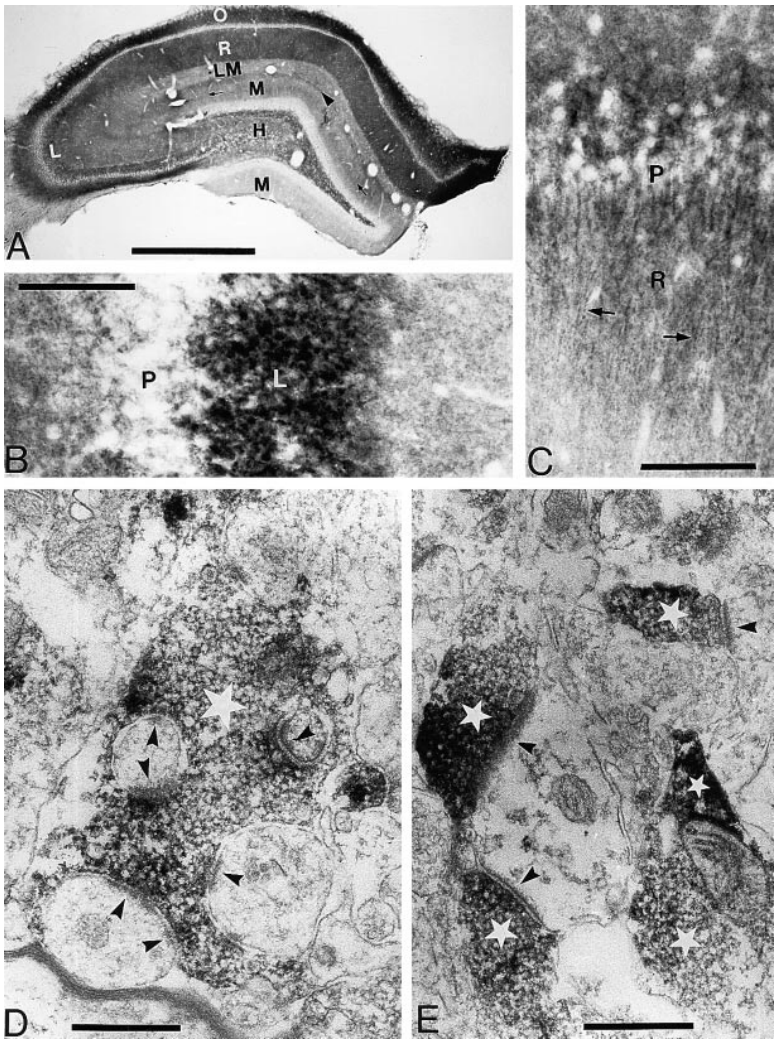

Figure 1. Munc13-1 Immunoreactivity in the Hippocampus

(A) Low-power view of the layer-specific distribution. L, stratum lucidum; O, stratum oriens; R, stratum radiatum; LM, stratum lacunosum-moleculare; M, molecular layer of dentate gyrus; H, Hilus of dentate gyrus. Arrow head, hippocampal fissure; arrows, border between inner and outer two-thirds of the molecular layer. Scale bar, 1 mm.

(B) In region CA3, the pyramidal cell layer (P) is unstained whereas the stratum lucidum (L) shows intensely stained patches of the same size and distribution as mossy fiber terminals. Scale bar, 50 μm.

(C) In region CA1, the cell bodies in the pyramidal cell layer (P) are unstained. In the stratum radiatum, there is a punctate pattern suggestive of presynaptic elements lining the surface of dendrites (arrows). Scale bar, 50 μm.

(D) A mossy fiber terminal (star) in stratum lucidum shows heterogeneous distribution of reaction product that appears densest close to the presynaptic membrane. Arrowheads point to active zones from the dendritic side. Scale bar, 0.5 μm.

(E) Numerous Munc13-1-positive small axon terminals in stratum radiatum of region CA1, same symbols as in (D). Scale bar, 0.5 μm.

isoforms, Munc13-2 and Munc13-3, are brain-specific mammalian homologs of the *C. elegans unc-13* gene product (Brose et al., 1995). Like their nematode counterpart, Munc13s are thought to regulate synaptic function. Munc13-1 interacts with syntaxin 1, an essential component of the synaptic release machinery involved in vesicle maturation and fusion (Betz et al., 1997), and with DOC2, a putative regulator of transmitter secretion (Orita et al., 1997). Beyond such fragmentary circumstantial evidence, the functional role of Munc13s (or that of unc-13p) in synaptic physiology is not known.

In the present study, we provide direct evidence for an involvement of Munc13-1 in presynaptic signaling. Our findings characterize Munc13-1 as a high-affinity phorbol ester receptor that is specifically localized to presynaptic transmitter release sites. Phorbol ester binding leads to the translocation of all Munc13 isoforms to the plasma membrane of transfected fibroblasts. Upon presynaptic overexpression in *Xenopus laevis* neuromuscular junctions, Munc13-1 acts as a phorbol ester–dependent enhancer of spontaneous and evoked neurotransmitter release. Our data establish Munc13-1 as an important presynaptic phorbol ester and diacylglycerol target that represents a second messenger pathway alternative to PKC.

Results

Localization of Munc13-1 in Rat Brain

All Munc13 isoforms are expressed in a brain-specific manner (Brose et al., 1995). However, their subcellular localization, or that of their *C. elegans* counterpart unc-13p, is not known. As morphological data on the localization of Munc13s are essential for further functional analysis, we studied the distribution of Munc13-1 in rat brain. For that purpose, a novel monoclonal antibody to Munc13-1 (clone 3H5) was generated and used in a detailed immunocytochemical analysis of rat hippocampus and cortex.

In hippocampus, a distinct layering of Munc13-1 immunostaining was observed. While layers containing pyramidal and granule cell bodies were devoid of signal, the degree of staining in the neuropil coincided with the layered distribution of termination areas of the different hippocampal axon systems (Figure 1A). Strongest signals were detectable in regions of highest presynaptic

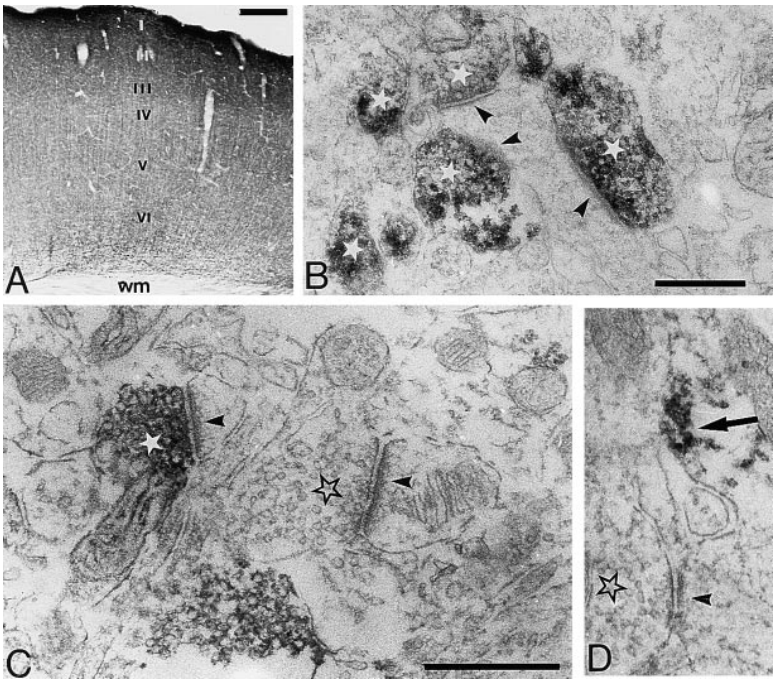

Figure 2. Munc13-1 Immunoreactivity in the Parietal Cortex

(A) A rather homogenous and dense labeling is found throughout laminae I to VI. The white matter (WM) is sparsely stained. Scale bar, 250 μm.

(B) Electron micrograph of a region with many Munc13-1-positive synapses (stars). Arrowheads point to active zones from the dendritic side. Scale bar, 0.5 μm.

(C) Two adjacent axo-spine synapses. One is formed by a Munc13-1-positive axon terminal (white star) and the other by a negative one (open star). Arrowheads point to active zones from the dendritic side. Scale bar, 0.5 μm.

(D) Munc13-1-positive material (arrow) beneath the plasma membrane of a dendrite that is postsynaptic to a Munc13-1-negative axon terminal (open star). Arrowheads point to active zones from the dendritic side. Scale bar as in C.

terminal density. In particular, strong patchy staining of mossy fiber terminals in stratum lucidum (Figure 1B) and punctate staining of presynaptic terminals in stratum radiatum (Figure 1C) were observed. Electron microscopic analysis demonstrated that most presynaptic boutons in the stratum radiatum were strongly stained (Figure 1E), whereas very little or no labeling of dendrites or dendritic spines was apparent. Likewise, all mossy fiber terminals in the stratum lucidum contained high amounts of Munc13-1 immunoreactivity that was concentrated at presynaptic release sites adjacent to postsynaptic densities (Figure 1D).

Like in the hippocampus, a prominent and dense punctate labeling in the neuropil, along with unstained pyramidal cell bodies in all cortical layers, indicated a predominantly presynaptic localization of Munc13-1 in the cerebral cortex (Figure 2A). This was confirmed under the electron microscope (Figures 2B and 2C). Compared to the hippocampus, the cortex contained a larger number of Munc13-1-negative synapses (Figure 2C). Quantification of immunostained synapses in randomly chosen micrographs demonstrated that only 45% of synapses in the parietal cortex are Munc13-1-positive (in contrast to 96% in the stratum lucidum and 56% in the stratum radiatum of the hippocampus). As a distinct cortical specialty, spots of Munc13-1 immunoreactivity were occasionally detected in apical dendrites of pyramidal cells where the reaction product was mostly confined to the vicinity of vesicular structures (Figure 2D). This dendritic labeling contributed less than 10% to the overall Munc13-1 immunoreactivity in the cortical neuropil, as estimated from randomly chosen electron micrographs, while essentially all other stained structures resembled presynaptic terminals.

In all brain regions, staining was abolished after preadsorption of the antibody to a Sepharose column coupled with the antigen used for immunization (data not shown).

Phorbol Ester Binding to Munc13-1

Our immunocytochemical analysis strongly suggested a presynaptic function of Munc13-1. In view of the possibility that unc-13p-like proteins might indeed serve as presynaptic diacylglycerol and phorbol ester receptors, we analyzed phorbol ester binding to Munc13-1 using a recombinant bacterial fusion protein encoding glutathione-S-transferase (GST) in frame with the Munc13-1 C_1-domain (Munc13-1C_1^{WT}; Figure 3A). The C_1-domain contains a Cys_6His_2 motif that forms a zinc finger structure (Hommel et al., 1994) and is responsible for phorbol ester binding in PKCs. The first His residue in the Cys_6His_2 motif (corresponding to His-567 in Munc13-1) is essential for phorbol ester binding in PKCs (Hommel et al., 1994; Quest et al., 1994).

Munc13-1C_1^{WT} bound the protein kinase C activator [^{3}H]4β-phorbol-12,13-dibutyrate ([^{3}H]4β-PDBu) with high specificity, while GST alone did not bind. Mutation of His-567 to Lys in the Cys_6His_2 motif of the C_1-domain abolished this binding (Munc13-1C_1^{H567}K; Figures 3B and 4A), indicating that the integrity of the zinc finger domain is essential for phorbol ester binding. The affinity of the Munc13-1 C_1-domain for [^{3}H]4β-PDBu was found to be similar to that of PKC (K_D = 5 nM; Figures 4B and 4C). Likewise, the pharmacological characteristics of phorbol ester binding to the Munc13-1 C_1-domain closely resembled those observed in PKC. Binding was inhibited by the putative endogenous ligand diacylglycerol (Figure 4D), by 4β phorbol esters like 4β-PDBu and 4β-12-O-tetradecanoylphorbol-13-acetate (4β-TPA), and by calphostin C, which all bind to the C_1-domain of PKCs as well. In addition, the rather nonspecific PKC inhibitor polymyxin B inhibited phorbol ester binding to Munc13-1. In contrast, commonly used control reagents that do not activate PKC (the 4α phorbol esters 4α-PDBu and 4α-TPA), and reagents that bind to the ATP binding site of PKC (bisindolylmaleimide), did not inhibit phorbol ester binding to the Munc13-1 C_1-domain (Figure 4E;

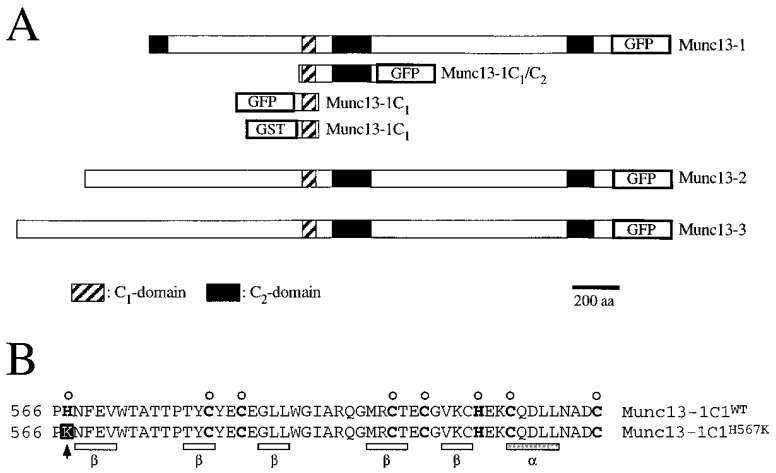

Figure 3. Munc13 Domain Structures and Expression Constructs

(A) Domain structures of full-length Munc13-1, Munc13-2, and Munc13-3, and representation of Munc13-1 fragments used for expression constructs. GFP, green fluorescent protein; GST, glutathione-S-transferase.

(B) Core Cys_6His_2 zinc finger motif of the Munc13-1 C_1-domain. Cys and His residues forming the zinc finger are indicated by open circles. WT, wild-type; H567K, mutation His-567 to Lys (indicated by arrow); α, α-helical region; β, β-strand region.

see Gordge and Ryves, 1994, for a review on PKC inhibitors and their specificity).

Phorbol Ester-Dependent Translocation of Munc13 Isoforms

Phorbol esters activate PKC by recruiting the enzyme to the plasma membrane (Newton, 1995, 1997; Sakai et al., 1997). To assay whether a similar phorbol ester-dependent translocation and activation of Munc13 takes place in a cellular environment, we studied the redistribution of transiently expressed Munc13 constructs in response to phorbol esters in a human fibroblast cell line (HEK293). For that purpose, we generated a series of mammalian expression constructs that encode fusion proteins of full-length Munc13-1, −2, or −3 with C-terminally attached green fluorescent protein (GFP; Figure 3A). HEK293 cells were transfected with these constructs and challenged with 100 nM 4β-TPA. We found that all three wild-type Munc13 isoforms translocated to the plasma membrane in response to 4β-TPA (Figure 5). In contrast, full-length Munc13-1^{H567K} (which carries the His-567Lys mutation and does not bind phorbol esters) was insensitive to 4β-TPA (Figure 5), indicating that phorbol esters mediate the translocation of Munc13 proteins in a PKC-independent manner by binding to the Munc13 C_1-domains.

To determine the minimal sequence of Munc13-1 that is required to mediate translocation, we expressed GFP fusion proteins of Munc13-1 fragments (Figure 3A). As translocation of PKC is dependent on both the C_1-domain and the C_2-domain, we first tested the phorbol ester–induced redistribution of the C_1/C_2 tandem domain of Munc13-1 (Munc13-$1C_1/C_2^{WT}$) and found that it translocated to the plasma membrane after stimulation with 4β-TPA, whereas the distribution of the corresponding His-567Lys mutation (Munc13-$1C_1/C_2^{H567K}$) was unaffected (Figure 6). In contrast, translocation of Munc13-$1C_1/C_2^{WT}$ as well as full-length Munc13-1^{WT} was not induced by Ca^{2+} ionophores (data not shown), supporting previous biochemical findings (Brose et al., 1995) and indicating that, unlike PKC, the C_2-domain of Munc13-1 does not induce Ca^{2+}-dependent membrane association. Rather, a single copy of a C_1-domain zinc finger is sufficient to mediate phorbol ester–dependent translocation in Munc13-1, as demonstrated by the redistribution of a Munc13-1 C_1-domain construct (Munc13-$1C_1^{WT}$) in response to 4β-TPA (Figure 6).

Role of Munc13-1 in Synaptic Transmission

Our morphological, biochemical, and cell biological analyses established Munc13-1 as a presynaptic high-affinity diacylglycerol and phorbol ester receptor. To evaluate a possible contribution of Munc13-1 to the diacylglycerol- or phorbol ester–dependent modulation of presynaptic efficacy, we examined the consequences of Munc13-1 overexpression in *Xenopus* neuromuscular junctions.

For that purpose, we injected mRNA encoding full-length Munc13-1^{WT} or Munc13-1^{H567K} (which carries the His-567 to Lys mutation and does not bind phorbol esters) together with GFP mRNA into early blastomeres of *Xenopus* and studied synaptic transmission in nerve-muscle cocultures prepared from the neural tube and associated myotomal tissue of injected stage 20–22 embryos. In each case, identical heterologous expression levels of Munc13-1^{WT} and Munc13-1^{H567K} were verified by Western blotting of individual injected and uninjected embryos from batches that were also used for coculture preparations (data not shown). Trains of six action potentials were elicited every 2–4 seconds in nerve cells by extracellular stimulation with a monopolar electrode or by current injection through the patch pipette in the current clamp mode. The resulting evoked postsynaptic currents (EPSCs) were recorded from the innervated muscle cells in the whole-cell configuration. After about 100 sec, 200 nM 4β-TPA was applied locally for 60 sec onto the area of nerve-muscle contact.

In a typical uninjected cell (Figure 7A), the EPSC amplitude increased sharply approximately 20 sec after the start of 4β-TPA application and reached its maximum after about 30 sec. Averaging the EPSC amplitude before and after application of 4β-TPA revealed an increase in the absolute EPSC amplitudes from 5.7 ± 1.8 nA to 8.5 ± 1.2 nA (mean ± s.d.), which corresponds to a 48% increase in relative synaptic transmission following phorbol ester application. Analysis of 19 noninjected

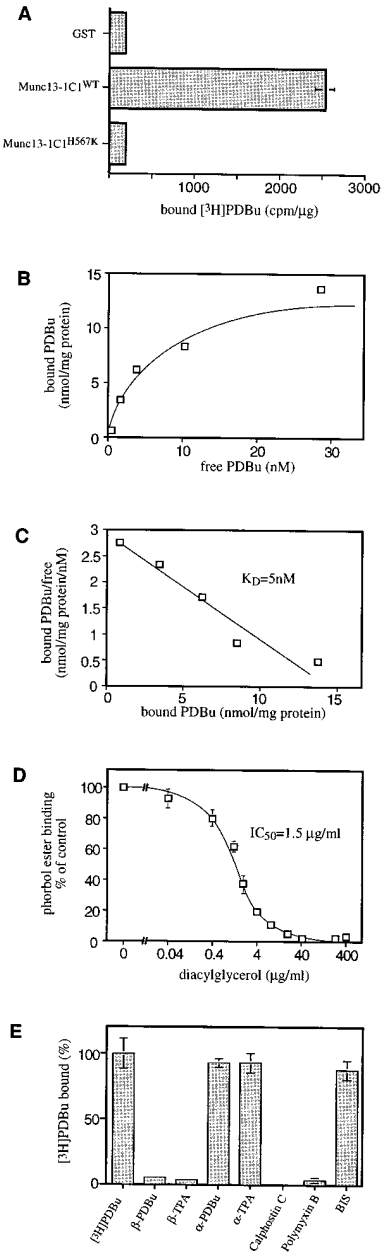

Figure 4. Phorbol Ester Binding to the Munc13-1 C_1-Domain

(A) Binding of ^{3}[H]4β-PDBu to wild-type Munc13-1 C_1-domain (Munc13-$1C_1^{WT}$) and mutated Munc13-1 C_1-domain (Munc13-$1C_1^{H567K}$). Proteins were used as GST fusion constructs. Binding of GST alone served as a negative control. Data are given as mean of double determinations (bar indicates range). Specific binding of ^{3}[H]4β-PDBu to the Munc13-1 C_1-domain is abolished by the His-567 to Lys mutation.

(B) Saturation binding of ^{3}[H]4β-PDBu to wild-type Munc13-1 C_1-domain (GST fusion construct).

(C) Scatchard analysis of saturation binding of ^{3}[H]4β-PDBu to wild-type Munc13-1 C_1-domain (GST fusion construct).

(D) Inhibition of ^{3}[H]4β-PDBu binding to wild-type Munc13-1 C_1-domain by diacylglycerol (GST fusion construct).

(E) Inhibition of ^{3}[H]4β-PDBu binding to wild-type Munc13-1 C_1-domain (GST fusion construct) by PKC ligands. α and β phorbol esters (PDBu and TPA), 1 μM; calphostin C, 20 μM; polymyxin B, 17.5 μM; bisindolylmaleimide (BIS), 3 μM.

Data are given as mean (B and C) or mean ± s.e.m. (A, D, and E) of double (A) or triple (B-E) determinations. Note that all ligands of PKC C_1-domains inhibit phorbol ester binding to the Munc13-1 C_1-domain, while the inactive α phorbol esters and bisindolylmaleimide (BIS, binds to the ATP binding site of PKC) do not.

cells demonstrated an average EPSC amplitude increase of 44.6 ± 4.5% (mean ± s.e.m.) after 4β-TPA application.

When the same protocol was applied to neuromuscular junctions of nerve cells overexpressing Munc13-1^{WT} (as identified by GFP fluorescence), we observed a strong increase in the responsiveness of synapses to phorbol esters. In the example illustrated in Figure 7B, local application of 200 nM 4β-TPA increased the average EPSC amplitude by 95% (7.7 ± 1.4 nA to 15 ± 3.1 nA; mean ± s.d.). Following a fast initial rise within the first 10 sec after 4β-TPA application, the amplitude reached a plateau after approximately 60 sec. Analysis of 13 Munc13-1^{WT}-injected cells demonstrated an average increase of 82.1 ± 12.9% (mean ± s.e.m.) in relative synaptic transmission following 4β-TPA application, compared to about 45% in control cells that did not express Munc13-1. This difference was statistically significant as determined by t-test ($p < 0.05$).

To demonstrate that the observed increase in relative synaptic transmission following Munc13-1^{WT} expression and phorbol ester stimulation is independent of PKC and exclusively due to phorbol ester binding by Munc13-1, we overexpressed Munc13-1^{H567K} in *Xenopus* embryos and analyzed synaptic transmission in the resulting neuromuscular junctions in culture. The His-567 to Lys mutation in Munc13-1^{H567K} abolishes phorbol ester binding to the Munc13-1 C_1-domain and prevents its phorbol ester–induced translocation to the plasma membrane (Figures 4, 5, and 6). Likewise, phorbol ester stimulation of synaptic transmission in neuromuscular junctions overexpressing Munc13-1^{H567K} was indistinguishable from that of uninjected control synapses (Figure 7C), although expression levels of Munc13-1^{H567K} were identical to those obtained for Munc13-1^{WT} (data not shown). Application of 200 nM 4β-TPA resulted in an average increase in relative transmitter release of 50% (Figure 7C), which was almost identical to that observed in control cells. Analysis of 11 Munc13-1^{H567K}-injected cells demonstrated an average increase of 42.1 ± 5.1% (mean ± s.e.m.) in relative synaptic transmission following 4β-TPA application, compared to about 45% in control cells that did not express Munc13-1 and 82.1 ± 12.9% in cells expressing Munc13-1^{WT} (Figure 7D). These data suggest that activation of the Munc13-1 C_1-domain by phorbol esters enhances neurotransmitter release.

We further characterized the shape and amplitudes of EPSCs recorded before 4β-TPA application from Munc13-1- and Munc13-1^{H567K}-injected neurons and compared them to those of uninjected control cells. As exemplified in the EPSC traces in Figures 7A, 7B, and 7C, there was no significant change in the overall shape of the EPSCs following Munc13-1 mRNA injection. Likewise, comparison of EPSC rise times and half-widths did not reveal any significant differences between control, Munc13-1- and Munc13-1^{H567K}-expressing neurons (data not shown). Table 1 summarizes the effects of Munc13-1 and Munc13-1^{H567K} expression on basal synaptic transmission. While there was no difference in the degree of paired pulse facilitation (which may serve as a measure for differences in release probability), the absolute EPSC amplitudes were somewhat larger, and coefficients of

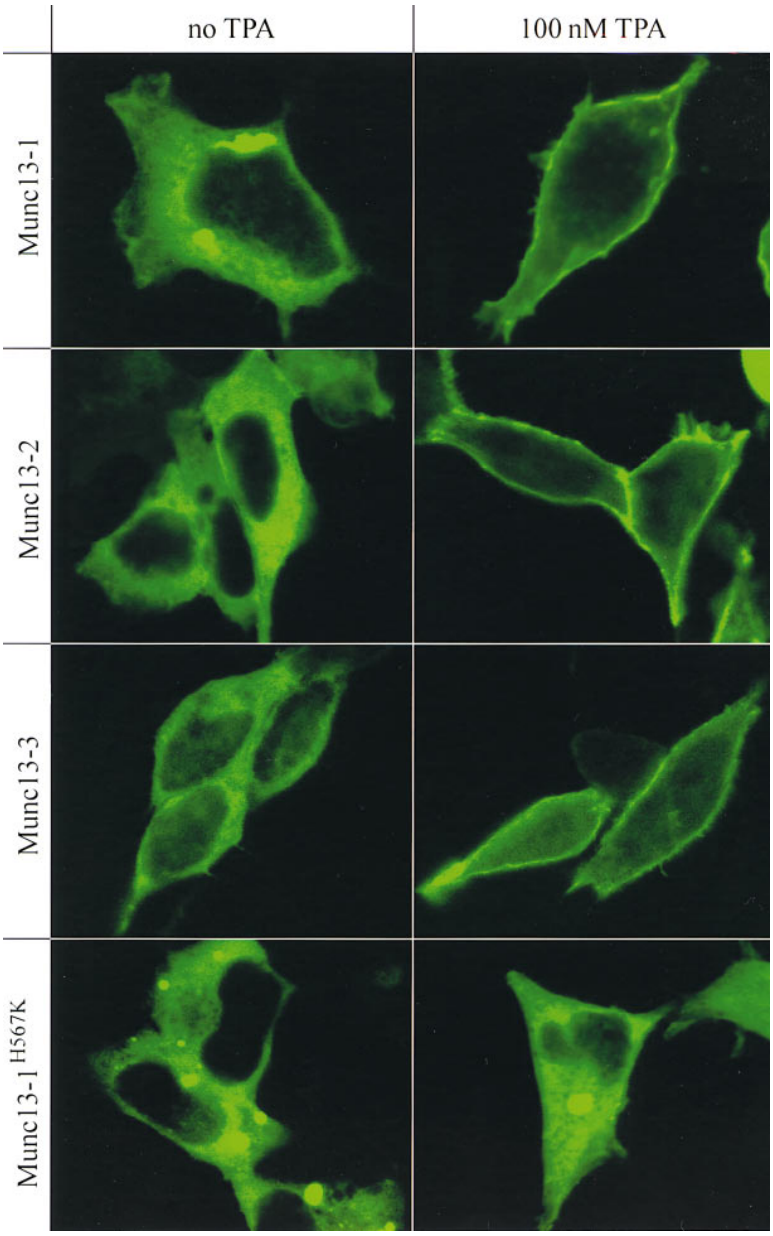

Figure 5. Phorbol Ester-Induced Translocation of Munc13 Isoforms

HEK293 cells were transfected with expression vectors encoding full-length Munc13-1, -2, and -3, as well as full-length Munc13-1^{H567K} (His-567 to Lys mutation in the C_1-domain, abolishing phorbol ester binding) with C-terminally attached GFP. Cells were either incubated in the presence of 100 nM 4β-TPA or kept under control conditions (no TPA), and the subcellular localization of expressed proteins was analyzed with a BioRad MRC 1024 confocal laser scanning microscope. Note that all wild-type Munc13 isoforms translocate to the plasma membrane in response to phorbol ester, whereas the phorbol ester insensitive full-length mutant Munc13-1^{H567K} does not.

variation (which reflect the variability of EPSC amplitudes) were slightly smaller in Munc13-1- and Munc13-1^{H567K}-expressing neurons as compared to control cells. These differences in basal synaptic transmission may indicate an increased quantal content in overexpressing cells (Table 1). However, the significance of this observation needs to be reexamined in a different experimental paradigm because an unequivocal interpretation of quantitative data is difficult in the *Xenopus* system that is characterized by a rather high variability of absolute ampitudes between cells/preparations.

An EPSC is often followed by a phase of asynchronous release that most likely reflects the increased release probability of single vesicles due to elevated calcium (Rahamimoff and Yaari, 1973). We recorded these as "spontaneous synaptic currents" (SSCs) for a duration of 1–3 sec immediately after the end of the last EPSC in a six pulse train and compared their frequency and amplitudes. Figure 8 depicts examples of SSCs collected immediately after the train in the absence or presence of 4β-TPA. The average frequency for control cells was 1.6 Hz before 4β-TPA application and increased to 2.4 Hz after 4β-TPA application (Figures 8A and 8B).

Munc13-1-injected cells exhibited an average SSC frequency of 3.8 Hz before 4β-TPA treatment, approximately 2.5 times higher than that of control cells. Following 4β-TPA application, the frequency increased to 7.2 Hz in Munc13-1-injected cells (Figures 8A and 8B). In contrast, the SSC frequency in cells expressing the mutant Munc13-1^{H567K} was not significantly elevated (Figures 8A and 8B). Average SSC amplitudes were slightly smaller in Munc13-1- and Munc13-1^{H567K}-expressing cells

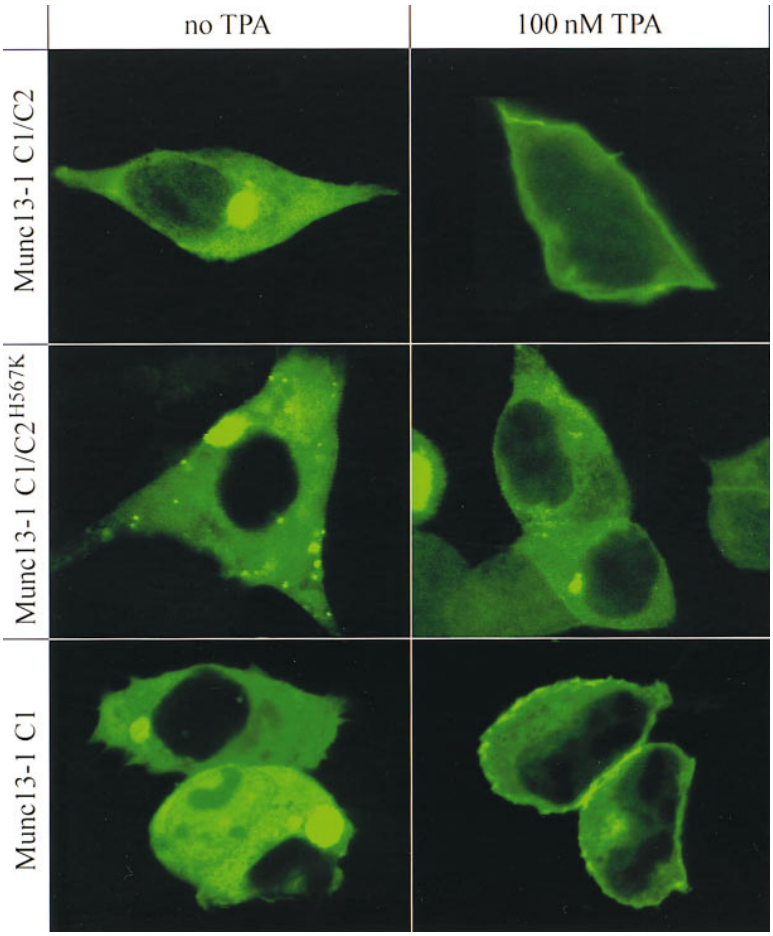

Figure 6. Phorbol Ester-Induced Translocation of Munc13-1 Is Mediated by the C_1-domain

HEK293 cells were transfected with expression vectors encoding fragments of Munc13-1 tagged with GFP. Cells were either incubated in the presence of 100 nM 4β-TPA or kept under control conditions (no TPA), and the subcellular localization of expressed proteins was analyzed with a BioRad MRC 1024 confocal laser scanning microscope. Munc13-1C1, Munc13-1 C_1-domain; Munc13-1C1/C2, Munc13-1 C_1C_2-tandem domain; Munc13-1C1/C2^{H567K}, Munc13-1 C_1C_2-tandem domain with His-567 to Lys mutation (abolishing phorbol ester binding). See Experimental Procedures for residues covered by these clones, and Figure 3 for their representation in the Munc13-1 domain structure. Note that the Munc13-1 C_1-domain is sufficient to mediate translocation in response to phorbol ester.

as compared to control cultures (Table 1). These results indicate that Munc13-1 also enhances the asynchronous release of synaptic vesicles by a mechanism that is largely dependent on the presence of an intact C_1-domain.

Discussion

Several indirect lines of evidence have identified Munc13 proteins as possible regulators of synaptic transmission: (1) Mutations in their *C. elegans* counterpart unc-13p lead to a paralyzed phenotype characterized by accumulation of neurotransmitter and resistance to acetylcholine esterase inhibitors, suggesting a deficit in transmitter release in these mutants (Hosono et al., 1987; Hosono and Kamiya, 1991); (2) the primary structures of Munc13 and unc-13 proteins contain C_1- and C_2-domains, indicating a regulation of Munc13/unc-13p function by diacylglycerol and calcium (Maruyama and Brenner, 1991; Ahmed et al., 1992; Kazanietz et al., 1995); (3) Munc13-1 interacts with syntaxin 1, a component of the synaptic release machinery involved in synaptic vesicle priming and fusion (Betz et al., 1997); and (4) Munc13-1 interacts with DOC2, a putative regulator of transmitter release, and influences DOC2-stimulated exocytosis from PC12 cells (Orita et al., 1997). In the present study, we provide direct evidence for an involvement of Munc13 proteins in presynaptic function.

Munc13-1 Is a Presynaptic Protein

Previous attempts to determine the precise localization of Munc13 proteins failed due to the poor specificity of the available antibodies in immunocytochemistry (Brose et al., 1995; Betz et al., 1997). For that reason, we generated a new isoform-specific monoclonal antibody to Munc13-1 (see Experimental Procedures) that was used to demonstrate an almost exclusively presynaptic localization of Munc13-1 (Figures 1 and 2). Our findings demonstrate that a first prerequisite supporting published conjectural claims of a presynaptic function of Munc13-1 and unc-13p, namely its appropriate localization, is indeed met.

Munc13-1 appears to be concentrated at synaptic active zones. In the large hippocampal mossy fiber terminals, Munc13-1 immunoreactivity was most prominent in presynaptic subcompartments that were opposite of postsynaptic densities (Figure 1). Given the limited diffusibility of the dye reaction product generated with our immunodetection method, these data suggest that Munc13-1 is concentrated at presynaptic release sites and not distributed uniformly in the presynaptic cytosol. Support for this view is provided by biochemical

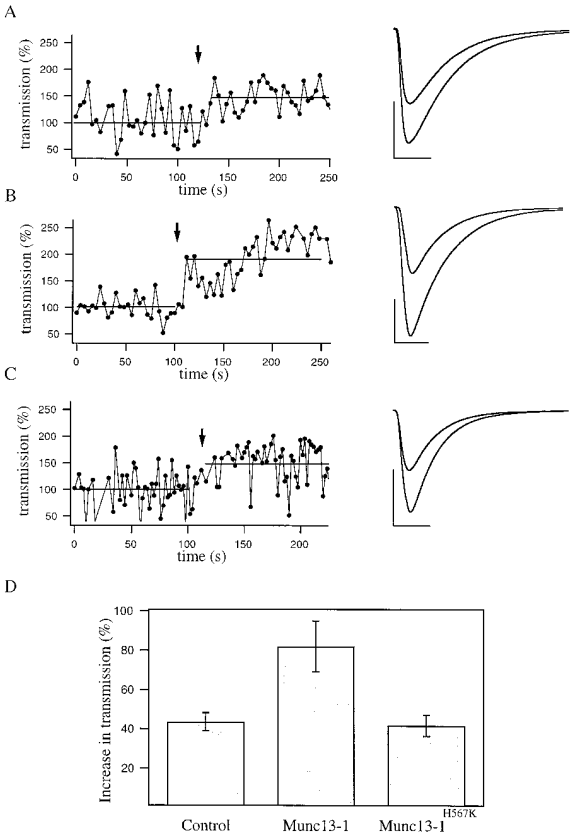

Figure 7. Phorbol Ester-Mediated Increase of Evoked Postsynaptic Currents Is Enhanced in Munc13-1-Injected Neuromuscular Junctions

(A–C) Neuromuscular cocultures from control embryos (A), from embryos injected with wild-type Munc13-1 mRNA (B), and from embryos injected with mRNA encoding Munc13-1^{H567K} (C) were analyzed as described. (Left) Normalized EPSC amplitudes from a control (A), Munc13-1-injected (B), and Munc13-1^{H567K}-injected (C) neuron before and after application of 200 nM 4β-TPA (arrow). Each data point (filled circle) represents the first EPSC amplitude out of a train of six or two stimuli given (see Experimental Procedures). (Right) An average EPSC (10 responses) before and after 4β-TPA application is shown on the right. The shapes of the EPSCs were not changed significantly. Scale bars, 5 msec; 4 nA.

(D) Relative increase in synaptic transmission in control neurons and in neurons injected with Munc13-1 or Munc13-1^{H567K} mRNA. The average increase in synaptic transmission following 200 nM 4β-TPA was 44.6 ± 4.8% in control cells (mean ± s.e.m.; n=19), 82.1 ± 12.9% in Munc13-1-injected neurons (mean ± s.e.m.; n=13), and 42.1 ± 5.1% (mean ± s.e.m.; n=11) in Munc13-1^{H567K}-injected neurons. The increase in transmission in Munc13-1-injected neurons was significantly higher than that observed in control and Munc13-1^{H567K}-injected cells (t-test, $p < 0.05$). The inactive phorbol ester 4α-PDBu was inactive in all cells tested (data not shown).

analyses that demonstrated that Munc13-1 is largely insoluble, most likely associated with components of the synaptic cytoskeleton, but not present on synaptic vesicles (Brose et al., 1995; Betz et al., 1997). However, an unequivocal determination of Munc13-1 localization within the presynaptic terminal can only be achieved with preembedding immunogold methods, which have so far been unsuccessful with our antibody.

Multiple Munc13-1-negative presynaptic terminals were observed in parietal cortex (55% of all observed terminals) and, to a lesser extent, in the stratum radiatum of the hippocamus (44% of all observed terminals). These percentages represent maximum values because limited antibody penetration contributes significantly to the number of unstained structures. However, our observations indicate that a significant number of synapses in cortex and hippocampus do not contain Munc13-1. We assume that these synapses contain Munc13-2 as in situ hybridization data demonstrate (I. A. and N. B., unpublished data) that Munc13-1 and Munc13-2 but not Munc13-3 are coexpressed in cortex and hippocampus of the rat.

The only exception to the presynaptic localization of Munc13-1 was observed in cerebral cortex. Here, about 10% of all Munc13-1-positive structures were localized in dendrites. In most cases, the Munc13-1 immunoreactivity was confined to the vicinity of vesicular structures (Figure 2D). It is possible that these postsynaptic Munc13-1-containing structures represent dendritic release sites (Piotte et al., 1985; Chazal and Ohara, 1986; Pucak and Grace, 1994).

Munc13 Proteins Are Phorbol Ester Receptors

The C_1-domains of the three known Munc13 isoforms are extremely homologous and contain all critical residues necessary for phorbol ester binding in PKCs (Kazanietz et al., 1994). Of the 51 residues that comprise the core Cys_6His_2 motif of the C_1-domain zinc finger, only two are different between the isoforms: Munc13-1 Ile-590 is replaced by Leu in Munc13-2 and Munc13-1 Thr-598 is replaced by Ser in Munc13-2 and by Leu in Munc13-3 (Betz et al., 1996). Because of this high homology, we assumed the biochemical characteristics of the three C_1-domains to be similar. We selected the C_1-domain of Munc13-1, the most abundant isoform (Brose et al., 1995), for a detailed analysis of phorbol ester binding.

Our binding data are in agreement with and extend previous studies on unc-13p (Maruyama and Brenner, 1991; Ahmed et al., 1992; Kazanietz et al., 1995). We demonstrate that phorbol ester binding to the Munc13-1 C_1-domain is virtually indistinguishable from that observed in PKCs. The phorbol ester affinity of the Munc13-1 C_1-domain (K_D = 5 nM; Figures 4B and 4C) is very similar to that of intact PKCs (K_D = 2.6 nM for PKCγ) and of isolated PKC C_1-domains (K_D = 3.4 nM for PKCγ C_1-domain) (Quest and Bell, 1994). Furthermore, the structural requirements for phorbol ester binding appear to be the same in Munc13-1 and PKC C_1-domains. Like in PKC (Quest et al., 1994), mutation of the first His residue in the Cys_6His_2 motif of Munc13-1 (His-567 to Lys) abolishes binding completely (Figures 3B and 4A), demonstrating that the integrity of the C_1-domain zinc finger is essential for phorbol ester binding.

In addition, the pharmacological characteristics of phorbol ester binding to Munc13-1 closely resemble the inhibitor profile described for PKC C_1-domains (Gordge and Ryves, 1994). Most importantly, diacylglycerol, an endogenous ligand for PKC C_1-domains, inhibits binding to the Munc13-1 C_1-domain with a potency comparable to that observed in PKC (Sharkey et al., 1984). Also, calphostin C, the most potent and most frequently used

Table 1. Basal Transmitter Release Characteristics in Munc13-1- and Munc13-1^{H567K}-Overexpressing Cultures before Phorbol Ester Treatment

	Control	Munc13-1	Munc13-1^{H567K}
EPSC amplitudes (nA)	3.94 ± 0.54 (37)	5.26 ± 0.71 (22)	6.7 ± 1.08 (15)
Coefficient of variation	0.36 ± 0.03 (37)	0.29 ± 0.03 (22)	0.287 ± 0.02 (15)
Paired pulse facilitation ratio	0.92 ± 0.03 (37)	0.90 ± 0.03 (22)	0.93 ± 0.03 (15)
SSC amplitudes (nA)	0.46 ± 0.06 (23)	0.36 ± 0.03 (12)	0.41 ± 0.08 (6)
SSC frequency (Hz)	1.6 ± 0.34 (23)	3.8 ± 0.64 (12)	2.3 ± 0.7 (6)
Quantal content (I/q)	8.5	14.6	16.3
Quantal content ($1/CV^2$)	7.7	11.8	12.1

Data are presented for control, Munc13-1-, and Munc13-1^{H567K}-overexpressing cells. I, mean EPSC amplitude; q, mean SSC amplitude; CV, coefficient of variation. Errors are given as standard error of the mean (s.e.m.); numbers in parentheses indicate the number of experiments.

C_1-domain antagonist, and the typically used PKC-activating 4β phorbol esters, inhibit binding (Figure 4E). In contrast, 4α phorbol esters (Figure 4E), which are often applied as inactive control reagents in PKC experiments, and C2-ceramide, a possible endogenous ligand of C_1-domains (data not shown), do not bind to the Munc13-1 C_1-domain.

These observations establish Munc13 proteins as novel phorbol ester targets whose most likely endogenous ligand is diacylglycerol. Our data imply that among the typically used control reagents in phorbol ester experiments on PKC (C_1-domain antagonists like calphostin C, inactive 4α phorbol esters, inhibitors of ATP binding like bisindolylmaleimide), only potent and selective inhibitors of ATP binding to PKC would allow one to distinguish phorbol ester–mediated effects on PKC from those on Munc13 proteins (assuming that Munc13s do not bind these ligands with a binding site outside the C_1-domain). In the past, a large number of studies investigating phorbol ester–mediated effects on PKC used control conditions that are inadequate in the light of the present findings (i.e., C_1-domain antagonists or inactive 4α phorbol esters; see Gordge and Ryves, 1994, for a recent review). Given the fact that ubiquitous Munc13 isoforms exist (GenBank entry AF020202; I. A., A. B., and N. B., unpublished data), conclusions drawn from those studies would have to be reevaluated for a possible involvement of Munc13 proteins if direct, PKC-independent effects of phorbol esters on these novel targets were demonstrated.

Phorbol Ester-Mediated Regulation of Munc13 Proteins Is Direct and Independent of PKC

Membrane translocation of PKCs in response to phorbol esters is a well established phenomenon (Newton, 1995, 1997; Sakai et al., 1997). Phorbol esters bind to the C_1-domain of PKCs and serve as hydrophobic anchors that recruit the enzyme to the plasma membrane, stabilize its active conformation, and increase its susceptibility to other second messengers (Newton, 1995, 1997). In order to investigate whether phorbol ester binding to Munc13 isoforms indeed has structural and functional consequences for these proteins, we studied the effects of phorbol ester treatment on the subcellular distribution of Munc13-1, -2, and -3 isoforms that were C-terminally tagged with GFP.

All three Munc13 isoforms, as well as the isolated Munc13-1 C_1-domain, translocate to the plasma membrane of HEK293 cells in response to phorbol esters (Figures 5 and 6). This effect is abolished in a Munc13-1 mutant that is unable to bind phorbol ester (Munc13-1^{H567K}; Figures 5 and 6). It can therefore not be dependent on PKC or a neuron-specific binding partner but must occur in response to a direct action of phorbol esters on the Munc13 C_1-domain. In certain PKC and synaptotagmin isoforms, membrane translocation or membrane binding can also be mediated by Ca^{2+}/phospholipid binding to the regulatory C_2-domains (Brose et al., 1992; Davletov and Südhof, 1993; Newton, 1995, 1997; Sakai et al., 1997). However, increasing the intracellular Ca^{2+} concentration by addition of a Ca^{2+} ionophore did not induce membrane translocation of full-length Munc13 isoforms or of Munc13-1 fragments containing the central C_2-domain (data not shown).

These data strongly suggest that ligand binding to the Munc13 C_1-domains has direct structural and functional consequences in a cellular environment. They result in a subcellular redistribution and membrane association of Munc13 proteins that may regulate an as yet unidentified enzymatic activity. In contrast, Munc13 C_2-domains may not function in Ca^{2+}/phospholipid signaling and Ca^{2+}-dependent membrane association.

Translocation of Munc13 isoforms in the synapse is likely to be modulated by additional mechanisms. In rat brain, Munc13-1 and −3 are largely insoluble (Brose et al., 1995; I. A., A. B., and N. B., unpublished data). Munc13-1 is specifically targeted to presynaptic active zones (Figures 1 and 2) by an unknown mechanism that may involve cytoskeletal components (Brose et al., 1995, unpublished data). Consequently, a diacylglycerol-dependent membrane association/dissociation cycle of Munc13-1 must take place in the microenvironment of the presynaptic release site. In contrast, rat brain Munc13-2 is mostly soluble (I. A., A. B., and N. B., unpublished data), and translocation in response to diacylglycerol is likely to produce more profound changes in the overall distribution of the protein.

Munc13-1 Is a Phorbol Ester-Dependent Enhancer of Transmitter Release

Our morphological, biochemical, and cell biological observations (Figures 1–6) suggest a role for Munc13-1 as a second messenger-dependent regulator of presynaptic function. To determine if Munc13-1 alters neurotransmitter secretion in response to phorbol esters, we overexpressed full-length Munc13-1^{WT} and the phorbol ester–insensitive mutant Munc13-1^{H567K} in *Xenopus* neuromuscular cocultures and analyzed the electrophysiological

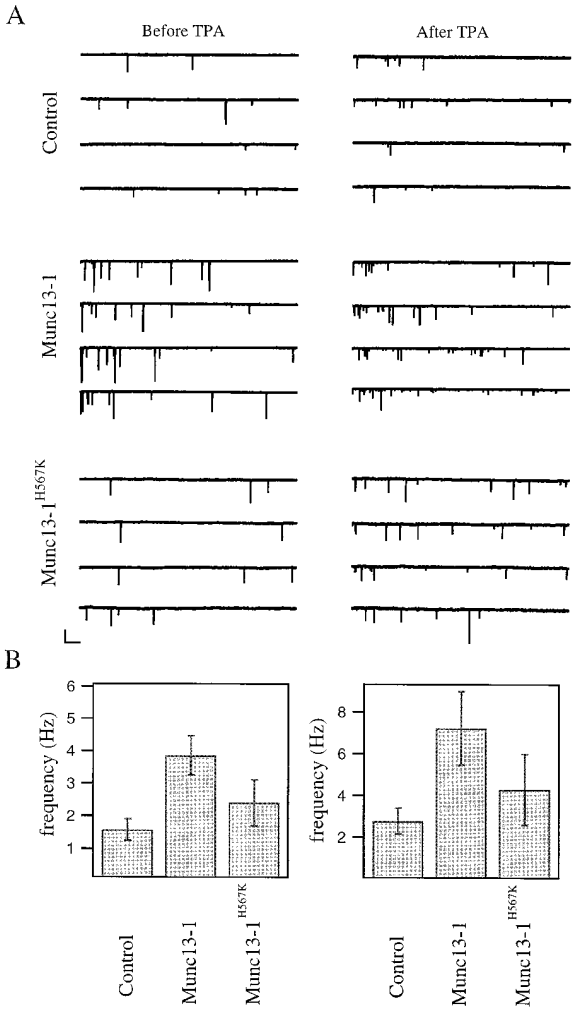

Figure 8. Overexpression of Munc13-1 Enhances the Frequency of Asynchronous Neurotransmitter Release in *Xenopus* Neuromuscular Junctions

(A) Representative traces of asynchronous release activity (SSCs) recorded from muscle cells that were innervated either by a control neuron (upper), a Munc13-1-overexpressing neuron (middle) or a Munc13-1^{H567K}-overexpressing neuron (lower). The left traces were recorded before and the right traces after 4β-TPA application (200 nM). The currents on the muscle cell are shown as downward deflections and represent single SSCs. Scale bars, 0.2 sec; 0.4 nA.

(B) Summary of SSC frequency in control neurons, Munc13-1-overexpressing neurons, and Munc13-1^{H567K}-overexpressing neurons before (left) and after 4β-TPA application (200 nM, right). The average SSC frequency for control cells was 1.6 Hz before and 2.4 Hz after 4β-TPA application. For Munc13-1-overexpressing neurons, the average frequencies were 3.8 and 7.2 Hz before and after 4β-TPA application, and for Munc13-1^{H567K}-overexpressing neurons the average frequencies were 2.4 and 4.2 Hz before and after 4β-TPA application. Data are given as mean ± s.e.m. of 23 (Control), 12 (Munc13-1) or 6 (Munc13-1^{H567K}) experiments. Differences in SSC frequencies between control and Munc13-1-overexpressing cells were statistically significant (t-test, $p < 0.05$).

characteristics of overexpressing synapses after phorbol ester treatment.

With respect to the question addressed in the present study, the *Xenopus* heterologous expression system has several advantages over other experimental paradigms. Proteins are expressed by the endogenous *Xenopus* protein synthesis machinery following injection of the respective mRNAs. This allows the expression of very large proteins, such as Munc13-1, which could otherwise not be synthesized in amounts sufficient for protein injection or that are too large for diffusion-based application through a patch pipette. Furthermore, generation and analysis of mutations are simple because sequence manipulations are performed on the cDNA level. Clearly defined mRNA constructs and their mutants can be introduced, allowing the design of optimal control conditions (point mutations, etc.). Finally, deleterious effects that may be associated with direct injections of peptides or proteins into presynaptic terminals are circumvented. The major disadvantage of the *Xenopus* neuromuscular coculture system is the fact that recorded responses can vary by a factor of 20 (0.5–10 nA, depending on the preparation/synapse examined), making a reliable quantitative analysis of absolute amplitude values almost impossible. We therefore concentrated in our analysis of Munc13-1 and Munc13-1^{H567K} overexpression on the relative effects of phorbol esters on transmitter release. *Xenopus* neuromuscular cocultures were used in the past to overexpress synapsin IIa (Schaeffer et al., 1994), synaptophysin (Alder et al., 1995), and frequenin (Olafsson et al., 1995).

When Munc13-1^{WT} mRNA is injected into *Xenopus* embryos, the resulting neuromuscular synapses show a higher susceptibility to phorbol esters than untreated junctions (Figure 7). This gain-of-function effect of Munc13-1^{WT} is specific for the overexpressed protein, dependent on an intact C_1-domain, and independent of PKC, as it is not observed when the phorbol ester–insensitive mutant Munc13-1^{H567K} is expressed at comparable levels (Figure 7).

A similar C_1-domain-dependent activity of Munc13-1 is also apparent on the level of SSCs following trains of stimuli. Here, Munc13-1^{WT} expression leads to an increase in the frequency of SSCs even in the absence of external phorbol esters. This effect is augmented when 4β-TPA is applied. In contrast, expression of the phorbol ester–insensitive mutant Munc13-1^{H567K} does not significantly affect SSC frequencies when compared to uninjected control cells (Figure 8).

These data indicate that Munc13-1 is a functional regulator of synaptic efficacy. Phorbol ester binding to the Munc13-1 C_1-domain or binding of residual membrane diacylglycerol in the case of synapses that were not treated with 4β-TPA appears to activate the protein, which in turn enhances transmitter release.

In addition to this, both Munc13-1 and Munc13-1^{H567K} overexpression lead to moderate increases in EPSC amplitudes and quantal content, indicating stimulatory effects of Munc13-1 on transmitter release that are independent of the intact C_1-domain. However, to verify these findings, a detailed study of the role of Munc13-1 in basal synaptic release has to be performed in a different experimental paradigm.

In principle, the observed changes in synaptic transmission due to Munc13-1 overexpression can be explained by (1) an effect of the protein on the structure

of synapses (e.g., the number of release sites per synapse), or by (2) an increased release-ready vesicle pool after Munc13-1 expression, or by (3) an effect of Munc13-1 on the release probability. Our data do not allow us to determine unequivocally the level at which Munc13-1 acts in the synaptic vesicle cycle. The fact that Munc13-1 overexpression does not alter paired pulse facilitation or the coefficient of variation suggests that the protein does not affect release probability (Table 1). Given its subcellular localization and biochemical characteristics, Munc13-1 is most likely to act on the release-ready vesicle pool at the level of the active zone. Munc13-1 interacts directly with the exocytotic core complex by binding to syntaxin (Betz et al., 1997), with DOC2 (Orita et al., 1997), and with components of the cytoskeleton (Brose et al., 1995, unpublished data). It is possible that these interactors recruit Munc13-1 to docked vesicles at the active zone. There, it would be activated by diacylglycerol in the plasma membrane either to promote vesicle docking or to perform a priming role, e.g., by altering the fusogeneity of the presynaptic plasma membrane or by affecting the stability of the core complex. To identify the locus of Munc13-1 action, the exact molecular or enzymatic function of Munc13-1 will have to be elucidated.

Conclusion

Munc13-1 is a high-affinity phorbol ester and diacylglycerol receptor localized in the presynaptic terminal. It represents a novel, PKC-independent target of the diacylglycerol second messenger pathway. Activation of Munc13-1 by phorbol esters induces its membrane association and enhances transmitter release. Munc13 proteins may be responsible for a number of phorbol ester effects on synaptic transmission and membrane traffic that cannot be attributed to PKC (Scholfield and Smith, 1989; Fabbri et al., 1994; Redman et al., 1997). The presence of Munc13-1 as a functional diacylglycerol and phorbol ester target at the active zone of the presynaptic terminal allows direct access for diacylglycerol second messengers to the transmitter release machinery, thereby adding a novel regulatory process to our understanding of synaptic transmission. Ubiquitous Munc13 isoforms may exert related functions in other tissues and cell types.

Experimental Procedures

Generation of Monoclonal Antibodies to Munc13-1

A monoclonal antibody to Munc13-1 was generated in collaboration with BioGenes (Berlin) using a fusion protein antigen encoding GST in frame with residues 1399–1736 of Munc13-1 (pGEX-Munc13-1F; Betz et al., 1997). The monoclonal antibody (clone 3H5) detects a single band of 200 kDa in Western blots of brain membranes and HEK293 cells transfected with pcDNA-Munc13-1 (Brose et al., 1995), which expresses full-length Munc13-1 (data not shown).

Immunocytochemistry

Adult, female Sprague-Dawley rats were anesthetized with ether and fixed by transcardial perfusion. Due to the sensitivity of the antigen recognized by the anti-Munc13-1 monoclonal antibody (clone 3H5), a nonstandard fixation scheme was applied. After flushing the vascular system with 0.9% NaCl (ca. 3 min), a fixative was perfused for 7 min that consisted of 4% unbuffered formalin, 0.9% NaCl, and 0.5% $ZnCl_2$. Thereafter, the animals were again perfused with 0.9% NaCl for 7 min to limit effects of postfixation. Brains were immediately dissected and cryoprotected with 30% sucrose. On a frozen microtome, 40 μm thick sections were cut for light and electron microcopic immunocytochemistry. The methods employed have been previously detailed (Rickmann and Wolff, 1995). In brief, after blocking unspecific antibody binding, anti-Munc13-1 monoclonal antibodies (clone 3H5) in ascites fluid were diluted 1:250 and applied for 12–16 hr at 37°C. These were detected with the ABC method (Vector Laboratories) followed by a histochemical nickel-intensified horseradish peroxidase reaction with 3,3′-diaminobenzidine. For electron microscopy, sections were osmicated and flat embedded. Only well reacted tissue (close to the surface of the incubated frozen sections) selected during double resectioning was used for the present investigation.

When a monoclonal antibody is used for immunostaining, the main sources of crossreactivity or artefactual staining are nonspecific antibodies and contaminating proteins in the ascites fluid. Therefore, control experiments were performed with (1) anti-Munc13-1 monoclonal antibody ascites fluid that had previously been preadsorbed to a Sepharose column coupled with the antigen used to generate the antibody and (2) secondary antibody alone. Under both conditions, staining of brain sections was completely abolished (data not shown). To exclude the possibility that our nonstandard fixation scheme gave rise to nonspecific staining, we performed additional control experiments with antibodies directed against GFAP. The resulting (predicted) glial labeling pattern was clearly different from the staining observed with the anti-Munc13-1 monoclonal antibody (data not shown), further demonstrating the specificity of our staining protocol.

Expression of Recombinant Proteins

Bacterial expression vectors encoding GST in frame with the Munc13-1 C_1-domain (Munc13-1C_1^{WT} and Munc13-1C_1^{H567K}; residues 556–651 of GenBank Acc. No. U24070) were generated in pGEX-KG using PCR fragments (Figure 3). Proteins were expressed and purified as described (Guan and Dixon, 1991). The mutation His-567 to Lys was generated by PCR, using primers that carried the appropriate coding sequence substitution (CAC to AAG at position 2807–2809 of the Munc13-1 cDNA).

Mammalian expression vectors encoding full-length Munc13-1^{WT}, Munc13-2, Munc13-3, and Munc13-1^{H567K} with a green fluorescent protein (GFP) sequence attached at their C termini were constructed in pEGFP-N1 (Clontech) using a combination of previously published cDNA fragments (Brose et al., 1995; GenBank Acc. No. U24070, U24071, and U24072) and engineered PCR fragments that ensured reading frame conservation (Figure 3). Constructs encoding the Munc13-1 C_1/C_2 tandem domain with a GFP sequence attached at its C terminus (Munc13-1C_1/C2^{WT} and Munc13-1C_1/C2^{H567K}; residues 556–826) were generated in pcDNA3-GFP (pcDNA3 from Invitrogen with EGFP insert) using PCR fragments that carried engineered Kozak consensus sequences and starter ATGs at the 5′ ends (Figure 3). The construct encoding the Munc13-1 C_1-domain with an N-terminally attached GFP sequence (Munc13-1C_1; residues 522–651 allowing a larger distance between GFP and the C_1-domain) was generated in pEGFP-C2 (Invitrogen) using a PCR fragment (Figure 3). The His-567 to Lys mutations were introduced by PCR (see above).

Munc13-1 vectors for use in *Xenopus* embryo expression experiments (Munc13-1^{WT} and Munc13-1^{H567K}) were generated in pCS2^{+} (Rupp et al., 1994) using inserts from a previously published full-length Munc13-1 cDNA (Brose et al., 1995). The His-567 to Lys mutation was generated by replacement of part of the wild-type sequence with a mutated cDNA fragment.

All PCR-based constructs were verified by dideoxy chain termination sequencing with dye terminators on an Applied Biosystems 373 DNA sequencer (Applied Biosystems). HEK293 cells were transfected with the above constructs using the calcium phosphate coprecipitation method (Chen and Okayama, 1987).

Phorbol Ester Binding Assays

Binding of [^{3}H]phorbol-12,13-dibutyrate ([^{3}H]4β-PDBu, 16 Ci/mmol; Amersham) to recombinant glutathione-S-transferase fusion proteins was measured according to Sharkey and Blumberg (1985).

[^{3}H]4β-PDBu (10 nM) was incorporated into liposomes (20% phosphatidylserine, 80% phosphatidylcholine, 300 μg/ml final concentration in assay; Avanti Polar Lipids) before addition to the assay. For that purpose, chloroform solutions of phosphatidylserine and phosphatidylcholine were evaporated under a stream of nitrogen. Dried lipids were resuspended in 50 mM Tris-HCl (pH 7.4) and 1 mM EGTA and sonicated for 40 sec with a Braun Labsonic U tip sonicator (Braun). Liposomes were centrifuged for 45 min at 3000 × gmax to remove aggregates and kept on ice until use. Nonspecific binding was determined in the presence of 30 μM unlabeled 4β-PDBu (Sigma). Saturation binding was assayed in the presence of increasing concentrations of [^{3}H]4β-PDBu (1–50 nM). Competition assays with diacylglycerol were carried out in the presence of increasing concentrations of 1,2-dioctanoyl glycerol (Avanti Polar Lipids). Competition assays with 4β-12-O-tetradecanoylphorbol-13-acetate (4β-TPA; Sigma), 4α-PDBu (Biomol), 4α-TPA (Biomol), Calphostin C (Calbiochem; light activated according to Fabbri et al., 1994), polymyxin B (Sigma), and bisindolylmaleimide (Sigma) were performed using the same procedure. Depending on the experiment, 0.3–3 μg protein were used per assay. Each data point represents the average of duplicate ([^{3}H]4β-PDBu binding to wild-type and mutated C_1-domain) or triplicate (other experiments) determinations. Each experiment was performed at least twice with essentially identical results.

Translocation Assays

HEK293 cells were grown on glass coverslips coated with 0.5% gelatine (Schnittler et al., 1993) and transfected with GFP expression vectors 2 days prior to the experiment. The media was changed before the experiment, and 4β-TPA (Sigma) was added from an aceton stock solution directly to the cell culture (100 nM final concentration). Cells were incubated for 5–60 min at 37°C, washed twice with phosphate-buffered saline, and fixed with 3% paraformaldehyde in phosphate-buffered saline. Cover slips were mounted onto slides with Fluoromount-G (Southern Biotechnology Associates) and observed with a MRC 1024 confocal laser scanning microscope (BioRad).

Preparation of Nerve-Muscle Cocultures

Xenopus nerve-muscle cocultures were prepared from the neural tube and associated myotomal tissue of stage 20–22 embryos as described (Tabti and Poo, 1991; Rettig et al., 1997). Following dissociation in $Ca^{2+}Mg^{2+}$-free solution (125 mM NaCl, 2 mM KCl, 1.2 mM EDTA, and 5 mM HEPES [pH 7.6]), cells were plated on glass coverslips pretreated for about 60 min with ECL (entactin, collagen and laminin; Upstate Biotechnologies) and grown for about 24 hr at 22°C. The culture medium consisted of 70% Leibovitz L-15 supplemented with GMS-X, antibiotics (Life Technologies), and BDNF (Alamone Labs). All electrophysiological experiments were carried out 1–2 days after plating.

mRNA Injection and Immunoblot Analysis

cDNAs of full-length Munc13-1, Munc13-1^{H567K}, and GFP were cloned into a pCS2$^+$ vector, linearized with NotI, and transcribed in vitro using SP6 RNA Polymerase (Boehringer Mannheim). The resulting mRNAs were suspended in RNAse-free H_2O to a final concentration of 2 μg/μl each for Munc13-1 and Munc13-1^{H567K} and 0.4 μg/μl for GFP. The mRNA for Munc13-1 or for Munc13-1^{H567K} was mixed with GFP mRNA, and approximately 10 nl of that mixture was pressure-injected into one blastomere of embryos at the 8- to 16-cell stage (Microinjector 5242; Eppendorf).

To determine whether the Munc13-1 constructs were functional, we performed immunoblot analyses on individual injected and noninjected embryos at different developmental stages following injection, using the monoclonal antibody to Munc13-1 (clone 3H5, see above). For this purpose, individual embryos were homogenized by trituration through Eppendorf tips with 100 μl of extraction buffer (150 mM NaCl, 5 mM EGTA, 0.2 mM phenylmethylsulfonyl fluoride, 1% Triton X-100, and 20 mM HEPES [pH 7.4]). Samples were centrifuged for 30 min at 15.000 × gmax at 4°C. The equivalent of 1/5 of a total embryo was analyzed by SDS-PAGE and Western blotting (Laemmli, 1970; Towbin et al., 1979; Brose et al., 1993), and immunoreactive bands were visualized by enhanced chemoluminescence (ECL; Amersham).

Both Munc13-1 and Munc13-1^{H567K} were readily detectable at similar levels in 2- and 3-day-old embryos (data not shown), indicating the presence of the proteins at times when electrophysiological measurements were performed. Likewise, GFP fluorescence was detected for several days after injection. As expected, noninjected embryos showed no rat Munc13-1 immunoreactivity.

Electrophysiological Recordings and Data Analysis

Prior to recording, spinal neurons were examined for GFP fluorescence. A monochromator-based illumination system (T.I.L.L. Photonics) was coupled into the epifluorescence port of an inverted IM 35 microscope (Zeiss) using a Fluar objective (40×, 1.3 N. A., oil immersion; Zeiss). Excitation wavelength for GFP was 488 nm, and the filter set was DC495, LP505 (T.I.L.L. Photonics).

GFP-containing fluorescent nerve cells were assumed to coexpress Munc13-1 or Munc13-1^{H567K}, respectively. Synaptic currents were recorded from innervated muscle cells in the whole-cell configuration using a combination of EPC-9 and EPC-7 amplifiers driven by the Pulse v8.06 software package (Heka Elektronik). The pipette solution for the muscle cells contained 107 mM CsCl, 1 mM $MgCl_2$, 1 mM NaCl, 10 mM EGTA, and 10 mM HEPES (pH 7.3). The bath solution contained normal frog ringer (NFR, 116 mM NaCl, 2 mM KCl, 1 mM $MgCl_2$, 1.8 mM $CaCl_2$, and 5 mM HEPES [pH 7.3]). The muscle cells were routinely clamped at −50 mV holding potential. A 10 ms test pulse to −60 mV was given before each EPSC sweep to estimate the series resistance for later offline series resistance compensation as previously described (Rettig et al., 1997). Action potentials were routinely elicited upon external stimulation (0.3–0.5 ms, 0.2–2 μA) on the nerve cell soma with frequencies of 0.5 Hz. Alternatively, the whole-cell configuration was established on the soma of the nerve cell, and the nerve cell was held at a potential between −50 and −70 mV in the current clamp mode. In current clamp mode, trains of six action potentials with an interval of 25 msec were elicited every 4 sec with 2 ms current injections of 900 pA. The pipette was filled with 114 mM K-gluconate, 10 mM KCl, 1 mM NaCl, 1 mM $MgCl_2$, 2 mM MgATP, 0.3 mM GTP, 50 μM fura-2, and 10 mM HEPES (pH 7.3). Amplitudes of EPSCs were analyzed with locally written software in IGOR (WaveMetrix, Inc.) as previously described (Rettig et al., 1997). No significant correlation was found between the initial amplitude and the effect of 4β-TPA. Spontaneous synaptic currents were recorded for a duration of 1–3 sec in experiments that were performed in the current clamp mode. SSC amplitudes and frequency were analyzed with locally written software in IGOR (WaveMetrix, Inc.). The inactive phorbol ester 4α-PDBu did not affect any of the cells tested (data not shown). Since we found no apparent differences in either SSC frequency or phorbol ester effect on EPSC amplitudes from Munc13-1-positive and Munc13-1-negative muscle cells, the data were grouped regardless of whether muscles cells were expressing Munc13-1 or Munc13-1^{H567K} or no exogenous protein (as judged by GFP coexpression).

Acknowledgments

We wish to thank I. Thanhäuser and F. Benseler for DNA synthesis and sequencing, S. Wenger, A. Neeb, and A. Bührmann for excellent technical assistance, F. Schmitz and T. Cole for advice on confocal microscopy, L. Stempka and W. Kittstein for advice on phorbol ester binding assays, C. Heinemann and V. Scheuβ for programming, and J. Ficner for artwork. This work was supported by the German Research Foundation (SFB406/A1 to N. B.; RE1092/3-1 to J. R.), by a Human Frontiers Science Program long-term fellowship (to U. A.), and by a Helmholtz fellowship (German Federal Ministry for Education and Research, to N. B.).

Received April 10, 1998; revised June 1, 1998.

References

Ahmed, S., Maruyama, I.N., Kozma, R., Lee, J., and Brenner, S. (1992). The Caenorhabditis elegans *unc-13* gene product is a phospholipid-dependent high-affinity phorbol ester receptor. Biochem. J. *287*, 995–999.

Alder, J., Kanki, H., Valtorta, F., Greengard, P., and Poo, M.-M. (1995). Overexpression of synaptophysin enhances neurotransmitter secretion at Xenopus neuromuscular synapses. J. Neurosci. *15*, 511–519.

Betz, A., Telemenakis, I., Hofmann, K., and Brose, N. (1996). Mammalian unc-13 homologues as possible regulators of neurotransmitter release. Biochem. Soc. Trans. *24*, 661–666.

Betz, A., Okamoto, M., Benseler, F., and Brose, N. (1997). Direct interaction of the rat unc-13 homologue Munc13-1 with the N-terminus of syntaxin. J. Biol. Chem. *272*, 2520–2526.

Brose, N., Gasic, G.P., Vetter, D.E., Sullivan, J.M., and Heinemann, S.F. (1993). Protein chemical characterization and immunocytochemical localization of the NMDA receptor subunit NMDA R1. J. Biol. Chem. *268*, 22663–22678.

Brose, N., Hofmann, K., Hata, Y., and Südhof, T.C. (1995). Mammalian homologues of C.elegans unc-13 gene define novel family of C_2-domain proteins. J. Biol. Chem. *270*, 25273–25280.

Brose, N., Petrenko, A.G., Südhof, T.C., and Jahn, R. (1992). Synaptotagmin: a Ca^{2+}-sensor on the synaptic vesicle surface. Science *256*, 1021–1025.

Byrne, J.H., and Kandel, E.R. (1996). Presynaptic facilitation revisited: state and time dependence. J. Neurosci. *15*, 425–435.

Chazal, G., and Ohara, P.T. (1986). Vesicle-containing dendrites in the nucleus raphe dorsalis of the cat. A serial section electron microscopic analysis. J. Neurocytol. *15*, 777–787.

Chen, C., and Okayama, H. (1987). High efficiency transformation of mammalian cells by plasmid DNA. Mol. Cell Biol. *7*, 2745–2752.

Cremona, O., and De Camilli, P. (1997). Synaptic vesicle endocytosis. Curr. Opin. Neurobiol. *7*, 323–330.

Davletov, B.A., and Südhof, T.C. (1993). A single C2-domain from synaptotagmin I is sufficient for high affinity Ca^{2+}/phospholipid binding. J. Biol. Chem. *268*, 26386–26390.

Dekker, L.V., De Graan, P.N.E., and Gispen, W.H. (1991). Transmitter release: target of regulation by protein kinase C? Progr. Brain Res. *89*, 209–226.

Fabbri, M., Bannykh, S., and Balch, W.E. (1994). Export of protein from the endoplasmatic reticulum is regulated by a diacylglycerol/phorbol ester binding protein. J. Biol. Chem. *269*, 26848–26857.

Gillis, K.D., Mößner, R., and Neher, E. (1996). Protein kinase C enhances exocytosis from chromaffin cells by increasing the size of the readily releaseable pool of secretory granules. Neuron *16*, 1209–1220.

Gordge, P.C., and Ryves, W.J. (1994). Inhibitors of protein kinase C. Cell. Signal. *6*, 871–882.

Guan, K.L., and Dixon, J.E. (1991). Eukaryotic proteins expressed in Escherichia coli: an improved thrombin cleavage and purification procedure of fusion proteins with glutathion-S-transferase. Anal. Biochem. *193*, 262–267.

Hanson, P.I., Heuser, J.E., and Jahn, R. (1997a). Neurotransmitter release—four years of SNARE complexes. Curr. Opin. Neurobiol. *7*, 310–315.

Hanson, P.I., Roth, R., Morisaki, H., Jahn, R., and Heuser, J.E. (1997b). Structure and conformational changes in NSF and its membrane receptor complexes visualized by quick-freeze/deep-etch electron microscopy. Cell *90*, 523–535.

Hay, J.C., and Scheller, R.H. (1997). SNAREs and NSF in targeted membrane fusion. Curr. Opin. Cell Biol. *9*, 505–512.

Hommel, U., Zurini, M., and Luyten, M. (1994). Solution structure of a cysteine rich domain of rat protein kinase C. Nat. Struct. Biol. *1*, 383–387.

Hosono, R., and Kamiya, Y. (1991). Additional genes which result in an elevation of acetylcholine levels by mutations in Caenorhabditis elegans. Neurosci. Lett. *128*, 243–244.

Hosono, R., Sassa, T., and Kuno, S. (1987). Mutations affecting acetylcholine levels in the nematode Caenorhabditis elegans. J. Neurochem. *49*, 1820–1823.

Kazanietz, M.G., Bustelo, X.R., Barbacid, M., Kolch, W., Mischak, H., Wong, G., Pettit, G.R., Bruns, J.D., and Blumberg, P.M. (1994). Zinc finger domains and phorbol ester pharmacophore. J. Biol. Chem. *269*, 11590–11594.

Kazanietz, M.G., Lewin, N.E., Bruns, J.D., and Blumberg, P.M. (1995). Characterization of the cysteine-rich region of the Caenorhabditis elegans protein Unc13 as a high affinity phorbol ester receptor. J. Biol. Chem. *270*, 10777–10783.

Laemmli, U.K. (1970). Cleavage of structural proteins during the assembly of the head of bacteriophage T4. Nature *227*, 680–685.

Maruyama, I.N., and Brenner, S. (1991). A phorbol ester/diacylglycerol-binding protein encoded by the *unc-13* gene of Caenorhabditis elegans. Proc. Natl. Acad. Sci. USA *88*, 5729–5733.

Newton, A.C. (1995). Protein kinase C: structure, function, and regulation. J. Biol. Chem. *270*, 28495–28498.

Newton, A.C. (1997). Regulation of protein kinase C. Curr. Opin. Cell. Biol. *9*, 161–167.

Olafsson, P., Wang, T., and Lu, B. (1995). Molecular cloning and functional characterization of the Xenopus Ca^{2+}-binding protein frequenin. Proc. Natl. Acad. Sci. USA *92*, 8001–8005.

Orita, S., Naito, A., Sakaguchi, G., Maeda, M., Igarashi, H., Sasaki, T., and Takei, Y. (1997). Physical and functional interactions of DOC2 and Munc13 in Ca^{2+}-dependent exocytotic machinery. J. Biol. Chem. *272*, 16081–16084.

Piotte, M., Beaudet, A., Joh, T.H., and Brawer, J.R. (1985). The fine structural organization of tyrosine hydroxylase immunoreactive neurons in rat arcuate nucleus. J. Comp. Neurol. *239*, 44–53.

Pucak, M.L., and Grace, A.A. (1994). Regulation of substantia nigra dopamine neurons. Crit. Rev. Neurobiol. *9*, 67–89.

Quest, A.F.G., and Bell, R.M. (1994). The regulatory region of protein kinase Cγ. J. Biol. Chem. *269*, 20000–20012.

Quest, A.F.G., Bardes, E.S.G., and Bell, R.M. (1994). A phorbol ester binding domain in protein kinase Cγ. J. Biol. Chem. *269*, 2961–2970.

Rahamimoff, R., and Yaari, Y. (1973). Delayed release of transmitter at the frog neuromuscular junction. J. Physiol. *228*, 241–257.

Redman, R.S., Searl, T.J., Hirsh, J.K., and Silinsky, E.M. (1997). Opposing effects of phorbol esters on transmitter release and calcium currents at frog motor nerve endings. J. Physiol. (Lond.) *501*, 41–48.

Rettig, J., Heinemann, C., Ashery, U., Sheng, Z.-H., Yokoyama, C.T., Catterall, W.A., and Neher, E. (1997). Alteration of Ca^{2+} dependence of neurotransmitter release by disruption of Ca^{2+} channel/syntaxin interaction. J. Neurosci. *17*, 6647–6656.

Rickmann, M., and Wolff, J.R. (1995). S-100 protein expression in subpopulations of neurons of rat brain. Neuroscience *67*, 977–991.

Rupp, R.A., Snider, L., and Weintraub, H. (1994). Xenopus embryos regulate the nuclear localization of XMyoD. Genes Dev. *8*, 1311–1323.

Sakai, N., Sasaki, K., Ikegaki, N., Shirai, Y., Ono, Y., and Saito, N. (1997). Direct visualization of the translocation of the γ-subspecies of protein kinase C in living cells using fusion proteins with green fluorescent protein. J. Cell. Biol. *139*, 1465–1476.

Schaeffer, E., Alder, J., Greengard, P., and Poo, M.-m. (1994). Synapsin IIa accelerates functional development of neuromuscular synapses. Proc. Natl. Acad. Sci. USA *91*, 3882–3886.

Schnittler, H.-J., Franke, R.P., Akbay, U., Mrowietz, C., and Drenkhahn, D. (1993). Improved in vitro rheological system for studying the effect of fluid shear stress on cultured cells. Am. J. Physiol. *265*, C289–C298.

Scholfield, C.N., and Smith, A.J. (1989). A phorbol diester-induced enhancement of synaptic transmission in olfactory cortex. Br. J. Pharmacol. *98*, 1344–1350.

Sharkey, N.A., and Blumberg, P.M. (1985). Highly lipophilic phorbol esters as inhibitors of specific [3H]phorbol 12,13-dibutyrate binding. Cancer Res. *45*, 19–24.

Sharkey, N.A., Leach, K.L., and Blumberg, P.M. (1984). Competitive inhibition by diacylglyerol of specific phorbol ester binding. Proc. Natl. Acad. Sci. USA *81*, 607–610.

Söllner, T.H., and Rothman, J.E. (1996). Molecular machinery mediating vesicle budding, docking and fusion. Experientia *52*, 1021–1025.

Südhof, T.C. (1995). The synaptic vesicle cycle: a cascade of protein-protein interactions. Nature *375*, 645–653.

Südhof, T.C., and Rizo, J. (1996). Synaptotagmins: C_2-domain proteins that regulate membrane traffic. Neuron *17*, 379–388.

Tabti, N., and Poo, M.-M. (1991). Culturing spinal neurons and muscle cells from Xenopus embryos. In Culturing Nerve Cells, G.Banker and K.Goslin, eds. (Cambridge, MA: MIT Press), pp. 137–154.

Towbin, H., Staehelin, T., and Gordon, J. (1979). Electrophoretic transfer of proteins from polyacrylamide gels to nitrocellulose sheets: procedure and some applications. Proc. Natl. Acad. Sci. USA *76*, 4350–4354.